



---

## Effects of Hematocrit on Impedance and Shear Stress during Stenosed Artery Catheterization

**V.P. Srivastava**

Director (Academic)  
Krishna Institute of Technology  
Kanpur-209217, India  
[vijai\\_sri\\_vastava@yahoo.co.in](mailto:vijai_sri_vastava@yahoo.co.in)

**Rati Rastogi**

Department of Mathematics  
S.V.N. Institute of Engineering  
Research and Technology, Barabanki-225003, India  
[ratirastogi1983@rediffmail.com](mailto:ratirastogi1983@rediffmail.com)

Received: September 15, 2008; Accepted: April 12, 2009

### Abstract

The flow of blood through a stenosed catheterized artery has been studied. To observe the effects of hematocrit, blood has been represented by a two-phase macroscopic model (i.e., a suspension of red cells in plasma). It is found that for any given catheter size, the impedance increases with hematocrit and also for a given hematocrit, the same increases with the catheter size. In the stenotic region, the wall shear stress increases in the upstream of the stenosis throat and decreases in the downstream in an uncatheterized artery but the same possesses an opposite character in the case of a catheterized artery. The shear stress at the stenosis throat possesses the character similar to the flow resistance (impedance) with respect to the hematocrit for a given catheter size, however, the same decreases with an increase in the size of the catheter for any given hematocrit.

**Key Words:** Stenosis; Hematocrit; Catheter; Impedance; Shear Stress; Erythrocytes

**MSC (2000) No.:** 76Z05

### 1. Introduction

Circulatory disorders are mostly responsible for over seventy five percent of all deaths and stenosis or arteriosclerosis is one of the frequently occurring diseases. Stenosis is the abnormal and unnatural growth in the arterial wall thickness that develops at various locations of the cardiovascular system under diseased conditions which occasionally results into the serious consequences. An account of most of the theoretical and experimental investigations on the subject may be had from Young (1979), Srivastava (1996, 2002), Sarkar

and Jayaraman (1998), Mekheimer and El-Kot (2008a, b). Arterial stenosis is associated with significant changes in the flow of blood, pressure distribution, wall shear stress and the flow resistance (impedance). The flow accelerates and consequently the velocity gradient near the wall region is steeper due to the increased core velocity resulting in relatively large shear stress on the wall even for a mild stenosis, in the region of narrowing arterial constriction. The flow rate and the stenosis geometry are the reasons for large pressure loss across the stenosis.

The increased impedance or the frictional resistance to flow and the wall shear stress will alter the velocity distribution when a catheter is inserted into a stenosed artery. A review of most of the experimental and theoretical investigations on artery catheterization has recently been presented by Srivastava and Srivastava (2008) in which they discussed the macroscopic two-phase blood flow through a catheterized artery of uniform diameter. Supported by experimental outcomes, Kanai (1970) established analytically that for each experiment, a catheter of appropriate size (diameter) is required in order to reduce the error due to the wave reflection at the tip of the catheter. A catheter with a tiny balloon at the end is inserted into the artery in balloon angioplasty to treat atherosclerosis. The catheter is carefully guided to the location at which stenosis occurs and balloon is inflated to fracture the fatty deposits and widen the narrowed portion of the artery. To measure translational pressure gradient during angioplasty procedures has been discussed by Gunj et al (1985), Anderson et al. (1986) and Wilson et al. (1988).

Leimgraber et al. (1985) have reported high mean pressure gradient across the stenosis. A catheter is composed of polyester based thermo plastic polyurethane, medical grade polyvinyl chloride, etc. The mathematical model corresponds to the flow through an annulus. Back (1994) and Back et al. (1996) studied the mean flow resistance increase during coronary artery catheterization in normal as well as stenosed arteries. The changed flow patterns of pulsatile blood flow in a catheterized stenosed artery were studied by Sarkar and Jayaraman (1998). Dash et al. (1999) further addressed the problem in a stenosed curved artery. Most recently, Sankar and Hemlatha (2007) studied the flow of Herschel-Bulkley fluid in a catheterized artery. The geometrically similar problem to observe the effects of an inserted catheter on uretral flow was analysed by Roos and Lykoudis (1970). Besides, several authors including Hakeem et al. (2002), Hayat et al. (2006) and Srivastava (2007) have explained the effects of an endoscope on flow behavior of chyme in gastrointestinal tract.

It is known that at low shear rates, blood being a suspension of corpuscles, behaves like a non-Newtonian fluid (Srivastava and Srivastava, 1983, 2008). Besides, the theoretical analysis of Haynes (1960) and the experimental observations of Cokelet (1972) indicate that blood can no longer be treated as a single-phase homogeneous viscous fluid in narrow arteries (of diameter  $\leq 1000 \mu m$ ). It is to note that the individuality of red cells (of diameter  $8 \mu m$ ) is important even in such large vessels with diameter up to 100 cells diameter (Srivastava and Srivastava (1983)). Skalak (1972) concluded that an adequate description of flow requires consideration of red cells as discrete particles. Certain observed phenomena in blood including Fahraeus-Lindqvist effect, non-Newtonian behavior, etc. can not be explained fully by treating the blood as a single-phase fluid. Thus, the individuality of erythrocytes (red cells) can not be ignored even while dealing with the problem of microcirculation. It appears to be therefore necessary and important to treat the whole blood as a particle-fluid (erythrocyte-plasma) mixture while flowing through narrow arteries.

The studies mentioned earlier on flow through stenosed catheterized vessels have considered blood either as a single-phase Newtonian or non-Newtonian fluid. Red blood cells are known to be responsible for many of the blood properties and diseases, and consequently dominate the flow field [Srivastava (1996)]. In large arteries such as aorta, the single-phase approach provides satisfactory tools to describe certain aspects, however, it fails to explain the behavior of blood while flowing through small diameter vessels [2400-8  $\mu\text{m}$ ; Srivastava and Srivastava (1983)]. With increasing applications of particulate suspension model to describe the flow behavior of blood in small diameter tubes, it is regretted that no efforts, at least to the authors knowledge has been made in the literature to observe the effects of hematocrit (volume fraction density of erythrocytes) on increased impedance, shear stress and other flow characteristics in stenosed catheterized arteries. We therefore propose to study the effects of hematocrit on flow behavior of blood while flowing through narrow stenosed catheterized arteries. The mathematical model considers the blood as an erythrocytes-plasma mixture (i.e., a suspension of erythrocytes in plasma).

## 2. Formulation of the Problem

Consider the axisymmetric flow of blood through a catheterized artery with an axisymmetric stenosis. The artery is assumed to be a rigid circular tube of radius  $R$  and the catheter as a coaxial rigid circular tube of radius  $R_1$ . The geometry of the stenosis which is assumed to be manifested in a catheterized arterial wall segment is described (Figure 1) as

$$\frac{R(z)}{R_o} = 1 - \frac{\delta}{2R_o} \left\{ 1 + \cos \frac{2\pi}{L_o} \left( z - d - \frac{L_o}{2} \right) \right\}; \quad d \leq z \leq d + L_o,$$

$$= 1 \quad \text{otherwise,} \quad (1)$$

with  $R(z)$  and  $R_o$  are the radius of the artery with and without stenosis, respectively,  $L_o$  is the stenosis length and  $d$  indicates its location.  $\delta = \delta_m(1 - e^{-t/\theta})$ , represents the instantaneous maximum height of the stenosis in which  $t$  is the time,  $\theta$  is the time constant, and  $\delta_m$  is the maximum projection of the stenosis in to the lumen. The parameters  $t$  and  $\theta$  are important only at the initial stages of the stenotic development and become insignificant as  $t \rightarrow \infty$  (Young, 1968).

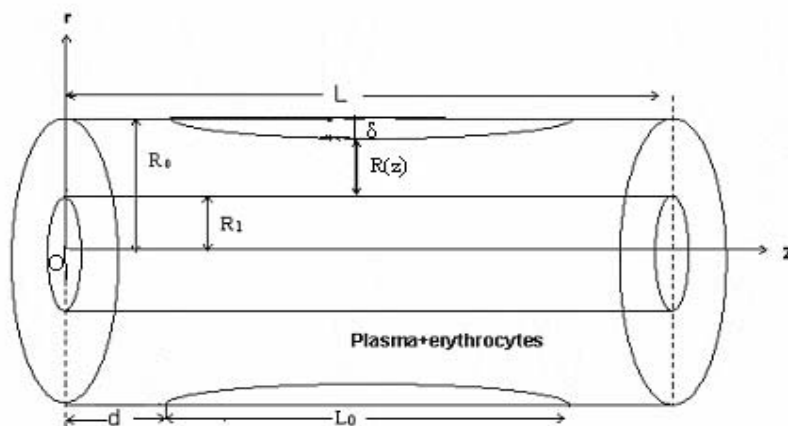


**Fig1. Flow geometry of an axisymmetric stenosis with an inserted catheter.**

Blood is assumed to be represented by a two-phase macroscopic model, that is, a suspension of erythrocytes (red cells) in plasma, a Newtonian viscous fluid. An attempt to analyze the problem in an exact manner seems to be very difficult due to the complicated structure of blood and the circulatory system. Under the simplified assumptions along with their justifications, stated in Srivastava and Srivastava (1983), the equations describing the steady flow of a two-phase macroscopic model of blood may be expressed as

$$(1-C)\rho_f \left\{ u_f \frac{\partial u_f}{\partial z} + v_f \frac{\partial u_f}{\partial r} \right\} = -(1-C) \frac{\partial p}{\partial z} + (1-C) \mu_s (C) \nabla^2 u_f + CS(u_p - u_f), \quad (2)$$

$$(1-C)\rho_f \left\{ u_f \frac{\partial v_f}{\partial z} + v_f \frac{\partial v_f}{\partial r} \right\} = - (1-C) \frac{\partial p}{\partial r} + (1-C) \mu_s (C) X(\nabla^2 - \frac{1}{r^2})v_f + CS(v_p - v_f), \quad (3)$$

$$\frac{1}{r} \frac{\partial}{\partial r} [r (1-C) v_f] + \frac{\partial}{\partial z} [(1-C)u_f] = 0, \quad (4)$$

$$C \rho_p \left\{ u_p \frac{\partial u_p}{\partial z} + v_p \frac{\partial u_p}{\partial r} \right\} = -C \frac{\partial p}{\partial z} + CS(u_f - u_p), \quad (5)$$

$$C \rho_p \left\{ u_p \frac{\partial v_p}{\partial z} + v_p \frac{\partial v_p}{\partial r} \right\} = -C \frac{\partial p}{\partial r} + CS(v_f - v_p), \quad (6)$$

$$\frac{1}{r} \frac{\partial}{\partial r} [r C v_p] + \frac{\partial}{\partial z} [C u_p] = 0, \quad (7)$$

where  $\nabla^2 \equiv (1/r) \partial/\partial r (r \partial/\partial r) + \partial^2/\partial z^2$  as Laplacian operator,  $r$  and  $z$  are the cylindrical polar coordinate system with  $z$  measured along the tube axis and  $r$  perpendicular to the axis of the tube.  $(u_f, u_p)$  and  $(v_f, v_p)$  are the axial and radial components of the (fluid, particle) velocity.  $\rho_f$  and  $\rho_p$  are the actual density of the material constituting the fluid (plasma) and the particle (erythrocyte) phases, respectively,  $(1-C)\rho_f$  is the fluid phase and  $C\rho_p$  is particle phase densities,  $C$  denotes the volume fraction density of the particles,  $p$  is the pressure,  $\mu_s(C) \approx \mu_s$  is the mixture viscosity (apparent or effective viscosity),  $S$  is the drag coefficient of interaction for the force exerted by one phase on the other, and the subscripts  $f$  and  $p$  denote the quantities associated with the plasma (fluid) and erythrocyte (particle) phase, respectively.

It is to note that the pressure gradients have been assumed to be the same for the two phases which is true in most of the practical situations [Drew (1976)]. The concentration of the particles is considered to be small enough as to neglect the field interaction among them [Srivastava (1996)]. The volume fraction density,  $C$  is also chosen constant which is a good approximation for the low concentration of small particles [Drew (1979); Srivastava et al. (1994)].

The expressions for the viscosity of suspension,  $\mu_s$  and the drag coefficient of interaction,  $S$  for the present problem have been chosen [Srivastava and coworker (1989; 1996)] as

$$\mu_s \cong \mu_s(C) = \frac{\mu_o}{1 - mC},$$

$$m = 0.07 \exp \left[ 2.49C + \left( \frac{1107}{T} \right) \exp(-1.69) \right], \quad (8)$$

$$S = 4.5 (\mu_o / a_o^2) \frac{4 + 3[8C - 3C^2]^{1/2} + 3C}{(2 - 3C)^2}, \quad (9)$$

where  $T$  is measured in absolute temperature ( $^{\circ}K$ ),  $a_o$  is the radius of a red cell and  $\mu_o$  is the plasma viscosity. The empirical relation for the suspension viscosity,  $\mu_s$  suggested by Charm and Kurland (1974), is found to be reasonably accurate up to  $C = 0.6$  (i.e., 60% hematocrit). One may recall here that hematocrit in human blood lies between 30% and 55%. Charm and Kurland (1974) tested equation (8) with a cone and plate viscometer and found it to be in agreement within 10% in the case of blood. Equation (9) derived by Tam (1969), represents the classical Stokes drag for small particle Reynolds number.

Due to the non-linearity of the convective acceleration terms, the solutions of equations (2)–(7) are formidable task. Depending on the stenosis size, however, certain terms in these equations are of less importance than others. Considering the case of a mild stenosis and under the conditions [Young (1968); Srivastava (2003)]:  $\delta/R_o \ll 1$ ,  $\text{Re}(2\delta/L_o) \ll 1$  and  $2R_o/L_o \approx o(1)$ ,  $\text{Re}$  being the tube Reynolds number; equations (2)–(7) are simplified to

$$(1 - C) \frac{dp}{dz} = (1 - C) \frac{\mu_s}{r} \frac{\partial}{\partial r} \left( r \frac{\partial}{\partial r} \right) u_f + CS (u_p - u_f), \quad (10)$$

$$C \frac{dp}{dz} = CS (u_f - u_p). \quad (11)$$

The boundary conditions are

$$u_f = 0 \text{ on } r = R(z),$$

$$u_f = 0 \text{ on } r = R_1, \quad (12)$$

### 3. Analysis

The integration of equations (10) and (11) under the boundary conditions (12), yields the expressions for the plasma,  $u_f$  and erythrocyte,  $u_p$  velocities as

$$u_f = - \frac{R_o^2}{4(1 - C) \mu_s} \frac{dp}{dz}$$

$$X \left\{ \left( \frac{R}{R_o} \right)^2 - \left( \frac{r}{R_o} \right)^2 - \frac{[(R/R_o)^2 - (R_1/R_o)^2]}{\log(R_1/R)} \log \left( \frac{r}{R} \right) \right\}, \tag{13}$$

$$u_p = - \frac{R_o^2}{4(1-C)\mu_s} \frac{dp}{dz} \left\{ \left( \frac{R}{R_o} \right)^2 - \left( \frac{r}{R_o} \right)^2 - \frac{[(R/R_o)^2 - (R_1/R_o)^2]}{\log(R_1/R)} \log \left( \frac{r}{R} \right) + \frac{4(1-C)\mu_s}{S R_o^2} \right\}. \tag{14}$$

The volumetric flow flux,  $Q$  is now calculated as

$$Q = 2\pi \int_{R_1}^R [r(1-C)u_f + rC u_p] dr$$

$$= - \frac{\pi R_o^4 [(R/R_o)^2 - \varepsilon^2] (dp/dz)}{8(1-C)\mu_s} \left\{ \left( \frac{R}{R_o} \right)^2 + \varepsilon^2 - \frac{[(R/R_o)^2 - \varepsilon^2]}{\log[(R/R_o)/\varepsilon]} + \beta \right\}, \tag{15}$$

with  $\varepsilon = R_1/R_o$  and  $\beta = 8C(1-C)\mu_s / S R_o^2$ , a non-dimensional suspension parameter.

The pressure drop,  $\Delta p$  (i.e.,  $p$  at  $z = 0$ ,  $-p$  at  $z = L$ ) across the stenosis is obtained as

$$\Delta p = \int_0^L \left( - \frac{dp}{dz} \right) dz$$

$$= \frac{8(1-C)\mu_s Q}{\pi R_o^4} \int_0^L F(z) dz, \tag{16}$$

with

$$F(z) = \frac{1}{\left\{ \left( \frac{R}{R_o} \right)^2 - \varepsilon^2 \right\} \left\{ \left( \frac{R}{R_o} \right)^2 + \varepsilon^2 - \frac{[(R/R_o)^2 - \varepsilon^2]}{\log[(R/R_o)/\varepsilon]} + \beta \right\}}.$$

The flow resistance (resistive impedance),  $\bar{\lambda}$  and the wall shear stress,  $\bar{\tau}_R$  are now calculated as

$$\bar{\lambda} = \frac{\Delta p}{Q} = \frac{8(1-C)\mu_s}{\pi R_o^4} G, \tag{17}$$

$$\bar{\tau}_R = \frac{R}{2} \frac{dp}{dz} = \frac{4(1-C)\mu_s Q}{\pi R_o^3} \left( \frac{R}{R_o} \right) F(z), \quad (18)$$

where

$$\begin{aligned} G &= \int_0^L F(z) dz \\ &= \int_0^d [F(z)]_{R/R_o=1} dz + \int_d^{d+L_o} F(z) dz + \int_{d+L_o}^L [F(z)]_{R/R_o=1} dz. \end{aligned} \quad (19)$$

The shearing stress,  $\bar{\tau}_s$  at the stenosis throat located at  $z = d + L_o/2$ , is thus obtained as

$$\bar{\tau}_s = \frac{4(1-C)(1-\delta/R_o)\mu_s Q}{\pi R_o^3 \left\{ (1-\delta/R_o)^2 - \varepsilon^2 \right\} \left\{ (1-\delta/R_o)^2 + \varepsilon^2 - \frac{[(1-\delta/R_o)^2 - \varepsilon^2]}{\log[(1-\delta/R_o)/\varepsilon]} + \beta \right\}}. \quad (20)$$

The first and the third integrals in the expression for  $G$  (equation (19)) are straight forward where as the analytical evaluation of the second integral is a formidable task. In view of this, one obtains the final expression for the flow resistance,  $\bar{\lambda}$  as

$$\bar{\lambda} = \frac{8(1-C)\mu_s}{\pi R_o^4} \left\{ \frac{L-L_o}{\eta} + \frac{L_o}{2\pi} \int_0^{2\pi} \frac{d\phi}{(\theta^2 - \varepsilon^2) \left\{ \theta^2 + \varepsilon^2 - (\theta^2 - \varepsilon^2) / \log(\theta/\varepsilon) + \beta \right\}} \right\}, \quad (21)$$

where

$$\begin{aligned} \theta &= \theta(\phi) = a + b \cos \phi, \quad a = 1 - \frac{\delta}{2R_o}, \\ \phi &= \pi - (2\pi/L_o)(z - d - L_o/2), \\ \eta &= (1 - \varepsilon^2) [1 + \varepsilon^2 + (1 - \varepsilon^2) / \log \varepsilon + \beta]. \end{aligned}$$

The expressions for the dimensionless flow resistance,  $\lambda$ , the wall shear stress,  $\tau_R$  and the shearing stress at the stenosis throat,  $\tau_s$  may now be written as

$$\lambda = (1-C)\mu \left\{ \frac{1}{\eta} \left( 1 - \frac{L_o}{L} \right) + \frac{L_o}{2\pi L} \int_0^{2\pi} \frac{d\phi}{(\theta^2 - \varepsilon^2) \left\{ \theta^2 + \varepsilon^2 - (\theta^2 - \varepsilon^2) / \log(\theta/\varepsilon) + \beta \right\}} \right\}, \quad (22)$$

$$\tau_R = (1-C)\mu \left( \frac{R}{R_o} \right) F(z), \quad (23)$$

$$\tau_s = \frac{(1-C)\mu(1-\delta/R_o)}{\left\{(1-\delta/R_o)^2 - \varepsilon^2\right\}\left\{(1-\delta/R_o)^2 + \varepsilon^2 - [(1-\delta/R_o)^2 - \varepsilon^2]/\log[(1-\delta/R_o)/\varepsilon] + \beta\right\}}, \quad (24)$$

where

$$\lambda = \bar{\lambda}/\lambda_o, \quad \tau_R = \bar{\tau}_R/\tau_o, \quad \tau_s = \bar{\tau}_s/\tau_o, \quad \mu = \mu_s/\mu_o,$$

$$\lambda = 8\mu_o L/\pi R_o^4, \quad \tau_o = 4\mu_o Q/\pi R_o^3,$$

$\lambda_o$  and  $\tau_o$  are resistive impedance and wall shear stress, respectively for an uncatheterized normal artery (no stenosis) in the absence of the particle phase.

Under the limit  $\varepsilon \rightarrow 0$  (no catheter), the expressions for the flow characteristics,  $\lambda$ ,  $\tau_R$  and  $\tau_s$  obtained in equations (22)-(24), take the form

$$\lambda = (1-C)\mu \left\{ \frac{1}{1+\beta} \left(1 - \frac{L_o}{L}\right) + \frac{L_o}{2\pi L} \int_0^{2\pi} \frac{d\phi}{\theta^2(\theta^2 + \beta)} \right\}, \quad (25)$$

$$\tau_R = \frac{(1-C)\mu}{(R/R_o)^3 + \beta(R/R_o)}, \quad (26)$$

$$\tau_s = \frac{(1-C)\mu}{(1-\delta/R_o)^3 + \beta(1-\delta/R_o)}, \quad (27)$$

which correspond to the macroscopic two-phase blood flow through an axisymmetric stenosis. In addition in the absence of particle phase, these expressions reduce to

$$\lambda = 1 - \frac{L_o}{L} + \frac{L_o}{L} \frac{2a^3 + 3ab^2}{2(a^2 - b^2)^{7/2}}, \quad (28)$$

$$\tau_R = \frac{1}{(R/R_o)^3}, \quad (29)$$

$$\tau_s = \frac{1}{(1-\delta/R_o)^3}, \quad (30)$$

which are the same results as derived in Young (1968) for the flow of a single-phase Newtonian viscous fluid through a circular tube with a mild stenosis.

### 3. Numerical Results and Discussion

In order to discuss the results of the study quantitatively, computer codes are developed to evaluate the analytical results obtained above numerically at the temperature of  $25.5^\circ\text{C}$  and some of the critical values are displayed graphically in figures. 2-9. The parameter values are selected as [Young (1968); Back (1994); Srivastava (2003)]  $a_o$  (radius of an erythrocyte) =

$8\mu\text{m}$ ;  $C$  (hematocrit %) = 0, 0.2, 0.4, 0.6;  $R_o$  (artery radius) = 0.01 cm;  $\delta/R_o$  (stenosis height) = 0, 0.05, 0.10, 0.15, 0.20;  $L_o$  (stenosis length, cm) = 1;  $L$  (artery length, cm) = 1, 2, 5;  $\varepsilon$  (catheter size) = 0, 0.1, 0.2, 0.3, 0.4, 0.5, 0.6. The present study corresponds to the particulate suspension of blood flow through an axisymmetric stenosis, to the flow through a normal catheterized artery and to the flow of a viscous Newtonian fluid for the parameter values,  $\varepsilon \rightarrow 0$ ,  $\delta/R_o = 0$  and  $C = 0$ , Respectively.

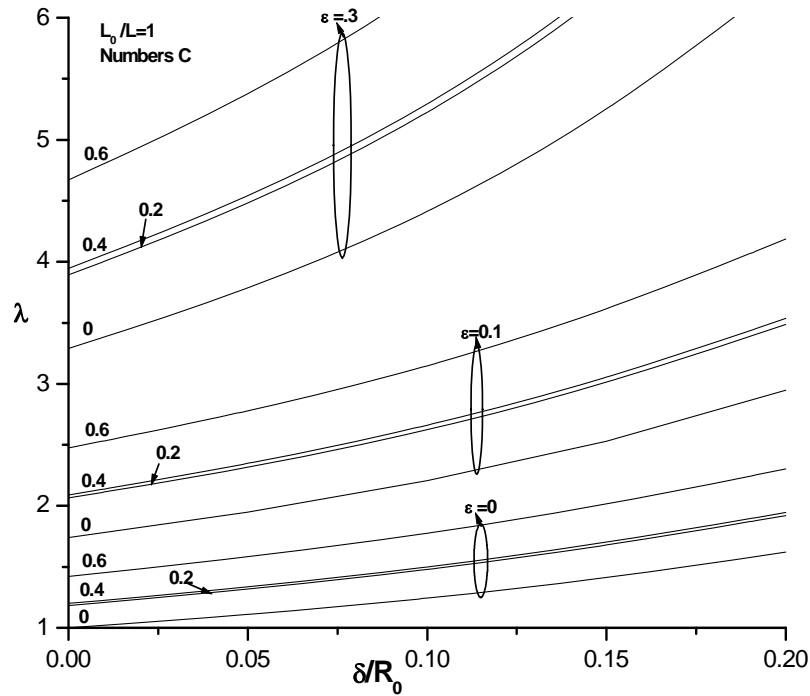


Fig.2 Variation of flow resistance,  $\lambda$  with  $\delta/R_o$  for different  $C$  and  $\varepsilon$ .

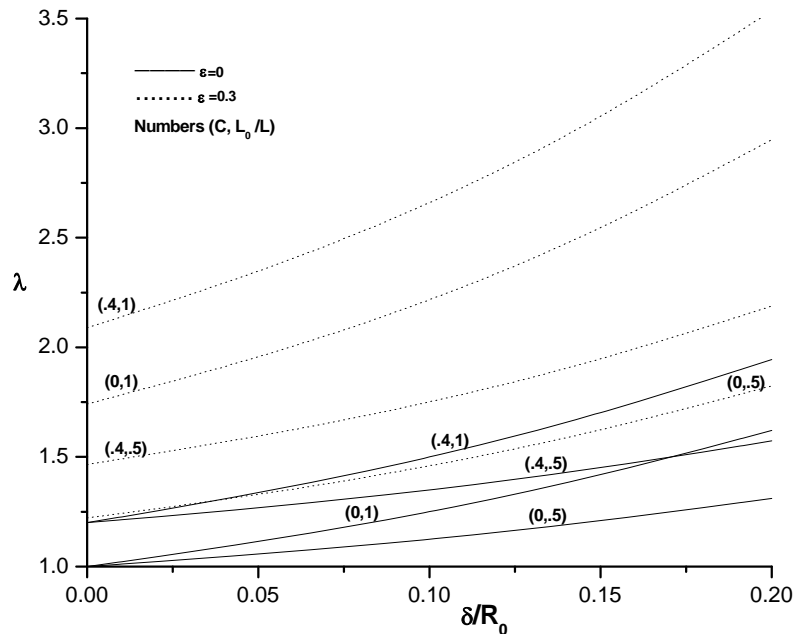


Fig.3 Variation of flow resistance,  $\lambda$  with  $\delta/R_0$  for different  $C, L_0/L$  and  $\varepsilon$ .

The flow resistance,  $\lambda$  increases with the stenosis height as well as with the hematocrit for any given catheter size,  $\varepsilon$ . It is noticed that for any given set of other parameters, the impedance increases with the catheter size  $\varepsilon$  (Figure 2). In addition,  $\lambda$  increases with the stenosis length,  $L_o$  (Figure 3). For a given hematocrit, even a small increase in the catheter size,  $\varepsilon$ , significant increase in the magnitude of the flow resistance,  $\lambda$  occurs (Figure 4). The blood flow characteristic  $\lambda$  steeply increases for small increasing values of the parameter,  $\varepsilon$  but increases rapidly for larger catheter size,  $\varepsilon$  (Figure 5).

The wall shear stress distribution,  $\tau_R$  in an uncatheterized artery increases from its approached magnitude (i.e., at  $z = 0$ ) in the upstream of the throat with the axial distance and achieves its maximal at the stenosis throat (i.e., at  $z = d + L_o/2$ ) and then decreases in the downstream and attains its approached magnitude at the end of the constriction profile (i.e. at  $z/L_o = 1$ ). Interestingly, however, the shear stress distribution,  $\tau_R$  possesses an opposite characteristics in a catheterized artery. The flow characteristic,  $\tau_R$ .

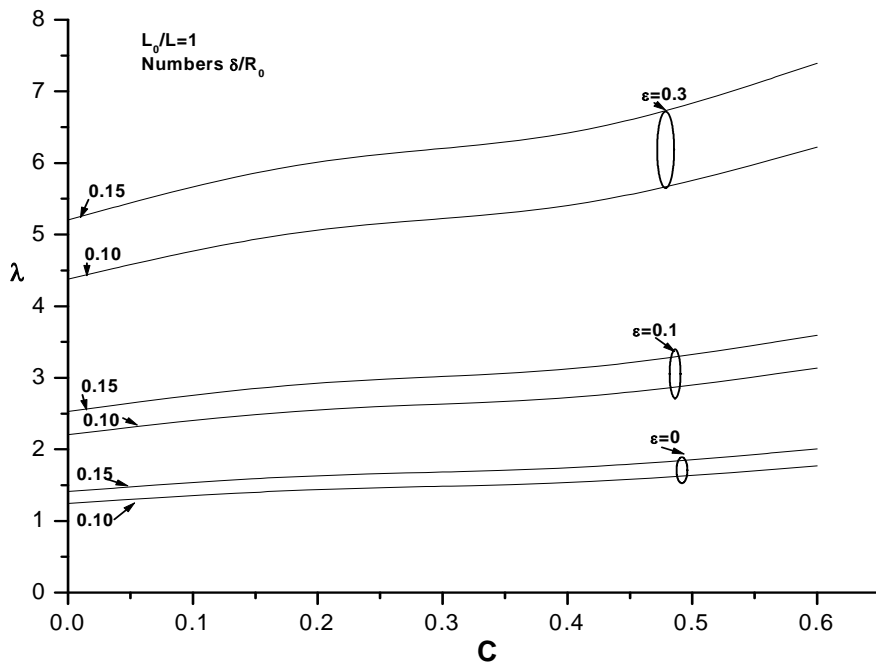


Fig.4 Variation of flow resistance,  $\lambda$  with  $C$  for different  $\delta/R_0$  and  $\epsilon$ .

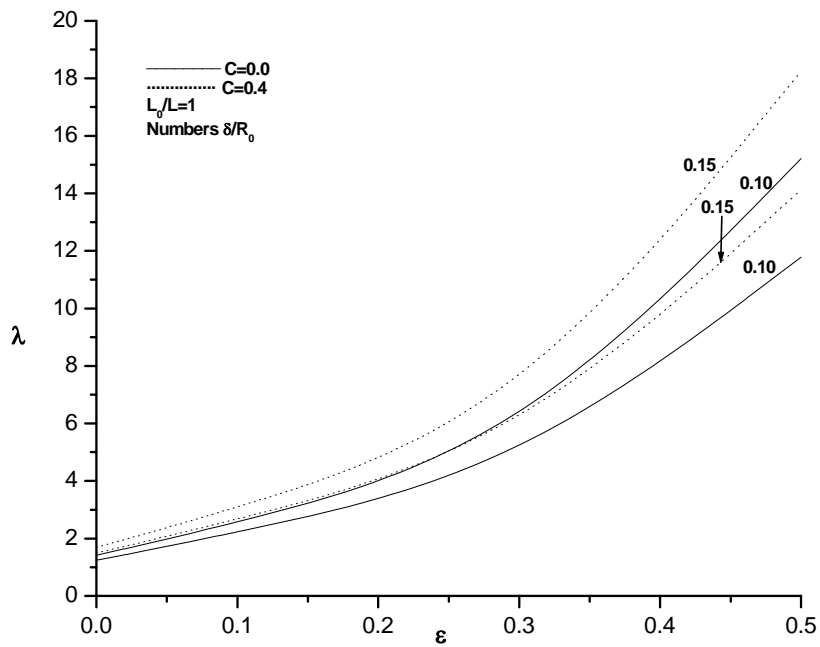


Fig.5 Variation of flow resistance,  $\lambda$  with  $\epsilon$  for different  $C$  and  $\delta/R_0$ .

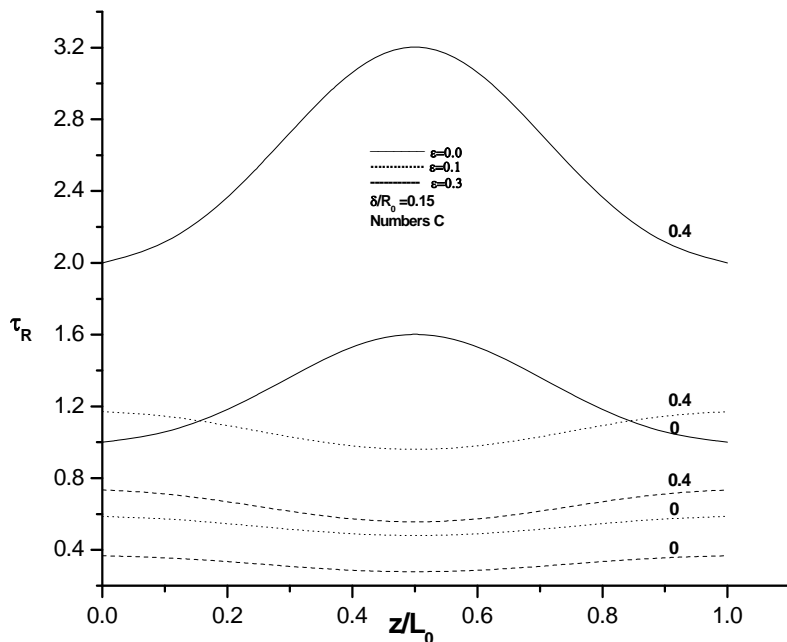


Fig.6 Wall shear stress,  $\tau_R$  distribution in stenotic region for different  $C$ ,  $\varepsilon$  and  $\delta/R_0$ .

decreases from its approached magnitude in the upstream, achieves its minimal at the throat and then increases in the downstream and attains its approached magnitude at the end of the constriction profile. One further notices that  $\tau_R$  decreases with increasing catheter size,  $\varepsilon$  for other parameters fixed (Figure 6).

Shearing stress at the stenosis throat,  $\tau_s$  increases with the stenosis size (height and length) for any given hematocrit  $C$  and the catheter size,  $\varepsilon$  (Figure 7).  $\tau_s$  increases with hematocrit,  $C$  for any given stenosis size and the catheter size,  $\varepsilon$  (Figure 8). The wall shear stress at the maximum height of the stenosis,  $\tau_s$  decreases with catheter size,  $\varepsilon$  for a given hematocrit. The flow characteristic,  $\tau_s$  assumes higher magnitude for higher stenosis height for small catheter size,  $\varepsilon$  [between  $\varepsilon = 0$  and 1.3 (approximately)] but the property reverses for large values of  $\varepsilon$  (Figure 9). One notices that  $\tau_s$  achieves an asymptotic magnitude when the catheter size becomes approximately fifty percent of the artery size.

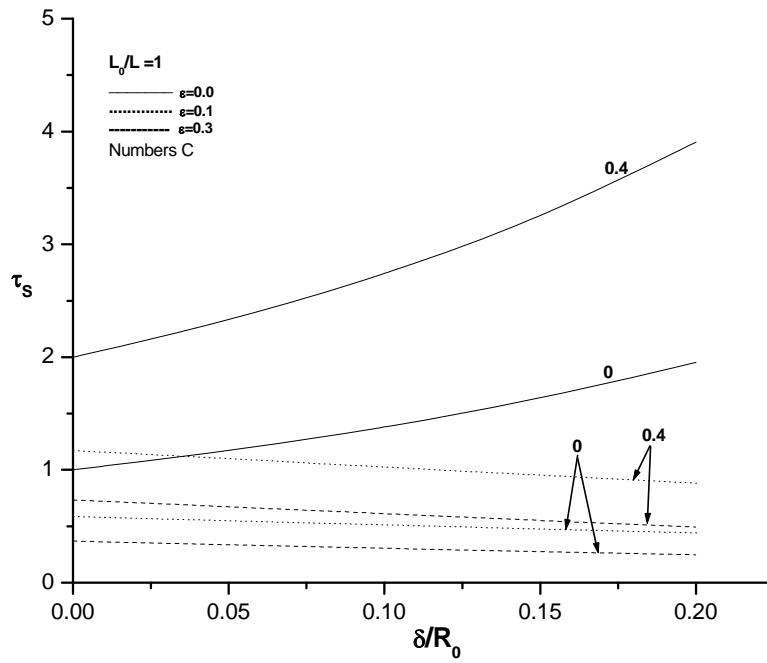


Fig.7 Variation of stress strain at stenosis throat,  $\tau_s$  with  $\delta/R_0$  for different C and  $\epsilon$ .

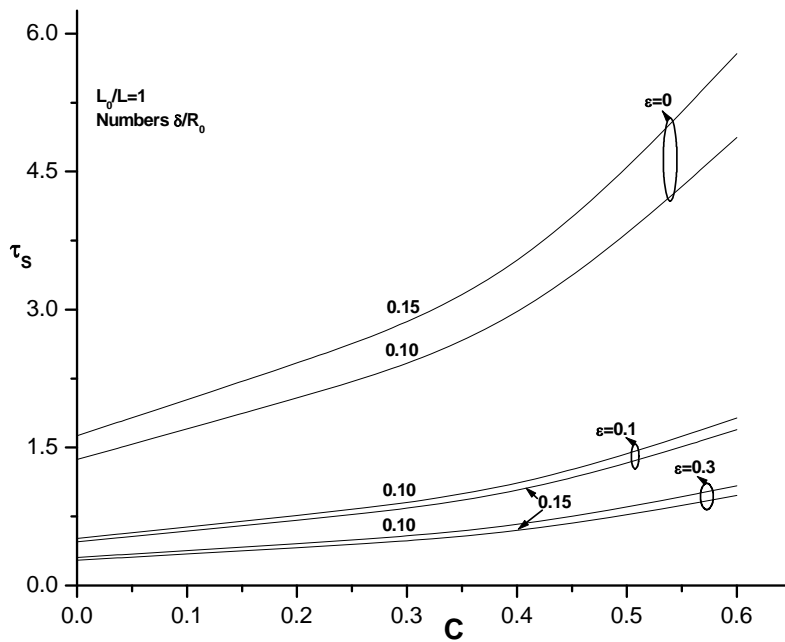


Fig.8 Variation of shear stress at stenosis throat,  $\tau_s$  with C for different  $\epsilon$  and  $\delta/R_0$ .

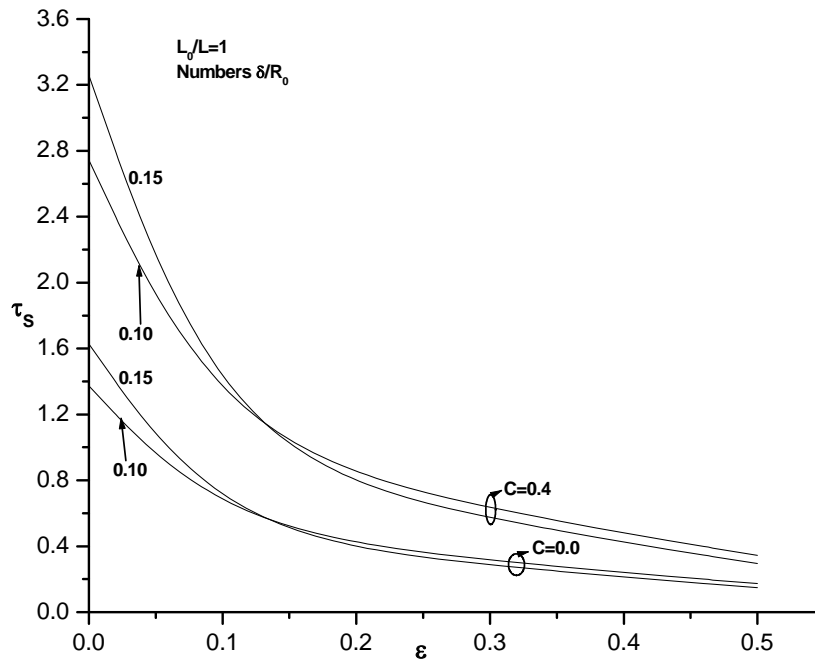


Fig.9 Variation of shear stress at stenosis throat for different  $C$  and  $\delta/R_0$ .

#### 4. Concluding Remarks

A macroscopic two-phase model of blood has been used to study the effects of hematocrit and the size of the inserted catheter on flow characteristics- impedance and shear stress in the stenotic artery. As mentioned earlier that in the absence of the catheter (i.e., under the limit  $\varepsilon \rightarrow 0$ ), the results of the present study reduces to the same as obtained in Srivastava (1995). The impedance increases with the increasing size of the catheter and assumes considerable higher magnitude in a catheterized artery (present study) than its corresponding magnitude in uncatheterized [Srivastava (1995)] for any given set of other parameters fixed. Also, for any given catheter size the impedance increases with hematocrit and with the stenosis size (height and length). The wall shear stress distribution in the stenotic region possesses almost an opposite characteristics in catheterized artery (present study) in comparison to its variations in an uncatheterized artery [Srivastava (1995)]. The variations in the magnitude of the shear stress at stenosis throat are observed having opposite characteristics in comparison to the variations in the magnitude of impedance (flow resistance).

#### Acknowledgements

Authors express sincere thanks to Prof. A. M. Haghghi, the Editor-in-Chief and the reviewers of the journal for their valuable comments and suggestions.

## REFERENCES

- Anderson, H.V., Roubin, G.S., Leimgruber, P.P., Cox, W.R., Douglas, Jr. J.S., King III, S.B. and Gruentzig, A.R. (1986). Measurement of Transstenotic Pressure Gradient during Percutaneous Tranluminal Coronary Angioplasty. *Circulation*, Vol. 73, pp. 1223-1230.
- Back, L.H. (1994). Estimated Mean Flow Resistance Increase during Coronary Artery Catheterization. *Journal of Biomechanics*, Vol. 27, pp. 169-175.
- Back, L.H., Kwack, E.Y. and Back, M.R. (1966). Flow Rate-Pressure Drop Relation in Coronary Angioplasty: Catheter Obstruction Effect. *Journal of Biomechanical Engineering*, Vol. 118, pp. 83-89.
- Charm, S.E. and Kurland, G.S. (1974). *Blood Flow and Microcirculation*. John Wiley, New York.
- Cokelet, G.R. (1972). The Rheology of Human Blood: In *Biomechanics, Its foundation and Objectives* (Ed. Y.C. Fung et al.), Prentice-Hall, Englewood Cliffs, N.J.
- Dash, R.K., Jayaraman, G. and Mehta, K.N. (1999). Flow in a Catheterized Curved Artery with Stenosis. *Journal of Biomechanics*, Vol. 32, pp. 49-61.
- Drew, D.A. (1976) Two-phase Flow: Constitutive Equations for Lift and Brownian Motion and Some Basic Flows. *Arch. Rat. Mechanics and Analysis*, Vol. 62, pp. 149-158.
- Drew, D.A. (1979). Stability of Stoke's Layer of a Dusty Gas. *Physics Fluids*, Vol. 19, pp. 2081-2084.
- Gunj, P., Abben, R., Friedman, P.L., Granic, J.D., Barry, W.H. and Levin, D.C. (1985). Usefulness of Transstenotic Coronary Pressure Gradient Measurements during Diagnostic Catheterization. *American Journal of Cardiology*, Vol. 55, pp. 910-914.
- Hakeem, A.E., Naby, A.E. and Misery, A.M.E. (2002). Effects of an Endoscope and Generalized Newtonian Fluid on Peristaltic Motion. *Applied Mathematics and Computation*, Vol. 128, pp.19-35.
- Hayat, T., Ali, N., Asghar, S. and Siddiqui, A.M. (2006). Exact Peristaltic Flow in Tubes with an Endoscope. *Appl. Math and Comput.* 182, pp. 359-368.
- Haynes, R.H. (1960). Physical Basis on Dependence of Blood Viscosity on Tube Radius. *American Journal of Physiology*, Vol. 198, pp. 1193-1205.
- Leimgruber, P.P., Roubin, G.S., Anderson, H.V., Bredlau, C.E., Whitworth, H. B., Douglas Jr., J.S., King III, S. B. and Gruentzig, A. R. (1985). Influence of Intimal Dissection on Restenosis after Successful Coronary Angioplasty, *Circulation*, Vol. 72, pp. 530-535.
- Mekheimer, Kh. S. and El-Kot. (2008a). Magnetic Field and Hall Currents Influences on Blood Flow through a Stenotic Artery. *Applied Mathematics and Mechanics*, Vol. 29, pp. 1-12.
- Mekheimer, Kh. S. and El-Kot. (2008b). The Micropolar Fluid Model for Blood Flow through a Taper Stenotic Arteries. *Acta Mecahnica Sinica*, DO/10.1007/s 10409-008-0185-7. In press.
- Roos, R. and Lykoudis, P.S. (1970). The Fluid Mechanics of the Ureter with an Inserted Catherter. *Journal of Fluid Mechanics*, Vol. 46, pp. 625- 630.
- Sakalak, R. (1972). *Mechanics of microcirculation: In Biomechanics,Its foundation and Objectives* (Ed. Y.C. Fung et al.), Prentice Hall, Englewood Cliffs.
- Sankar, D.S. and Hemlatha, K. (2007). Pulsatile Flow of Hersche-I-Bulkley Fluid through Catheterized Arteries-A Mathematical Model. *Appllied Mathematical Modelling*, Vol. 31, pp. 1497-1517.
- Sarkar, A. and Jayaraman, G. (1998). Corretion to Flow Rate-pressure Drop in Coronary Angioplasty; Steady Streaming Effect. *Journal of Biomechanics*, Vol. 31, pp. 781-791.

- Srivastava, L.M. and Srivastava, V.P. (1983). On Two-phase Model of Pulsatile Blood Flow with Entrance Effects, *Biorheology*, Vol. 20, pp. 761-777.
- Srivastava, L.M. and Srivastava, V.P. (1989). Peristaltic Transport of a Particle-fluid Suspension, *Journal of Biomechanical Engineering*, Vol. 111, pp. 157-165.
- Srivastava, L.M., Edemeka, U.E. and Srivastava, V.P. (1994). Particulate Suspension Model for Blood Flow Under External Body Acceleration. *International Journal of Biomedical Computing*, Vol. 37, pp. 113-129.
- Srivastava, V. P. (1995). Particle-fluid Suspension Model of Blood Flow through Stenotic Vessels with Applications. *International Journal of Bio-Medical Computing*, Vol. 38, pp. 141-154.
- Srivastava, V.P. and Srivastava, Rashmi. (2009). Particulate Suspension Blood Flow through a Narrow Catheterized Artery, *Computer and Mathematics with Applications*, In press.
- Srivastava, V.P. (2007). Effects of an Inserted Endoscope on Chyme Movement in Small Intestine. *Applications and Applied Mathematics*, Vol. 2, pp. 79-91.
- Srivastava, V.P. (2002). Particulate Suspension Blood Flow through Stenotic Arteries: Effects of Hematocrit and Stenosis Shape. *Indian Journal of Pure and Applied Mathematics*, Vol. 33, pp.1353-1360.
- Srivastava, V.P. (1996). Two-phase Model of Blood Flow through Stenosed Tubes in the Presence of a Peripheral Layer. *Applications, Journal of Biomechanics*, Vol. 29, pp. 1377-1382.
- Tam, C.K. W. (1969). The Drag on a Cloud of Spherical Particles in Low Reynolds Number Flows. *Journal of Fluid Mechanics*, Vol. 38, pp.537-546.
- Wilson, R. F., Johnson, M. R., Marcus, M.L., Aylward, P. E. G., Skorton, D. J., Collins, S. and White, C. W. (1998). The Effect of Coronary Angioplasty on Coronary Flow Reserve, *Circulation*, Vol. 77, pp. 873-885.
- Young, D. F. (1968). Effects of a Time-dependent Stenosis of Flow through a Tube. *Journal of Eng. Ind.*, Vol. 90, pp. 248-254.